

# Development of Mathematical Models for Blast Furnaces

Koki NISHIOKA\*  
Kouji TAKATANI

Yutaka UJISAWA

## Abstract

*Complicated phenomena take place in a blast furnace: raw materials are charged into it, and while gradually descending, they undergo chemical reactions and phase transformations. Mathematical models for blast furnaces have been developed: one is a three-dimensional unsteady state model to express the operation behavior of a blast furnace, and the other is a model for estimating the wear and erosion of the hearth wall and bottom bricks. With these models, it is now possible to express conditions inside the furnace at steady operation, follow the same unsteady operation after blow-in, and predict the erosion of the hearth wall and bottom bricks. They are proving instrumental for analyzing the actual operation of blast furnaces.*

## 1. Introduction

Different types of materials of a wide variety of components exist inside a blast furnace in the forms of gas, liquid, solid, and powder, a great number of reactions take place there as illustrated in Fig. 1, and those phenomena are influenced by many factors such as gas flow, chemical reactions, burden descent, the resistance to gas and liquid flow, and the shape of the cohesive zone. As complicated as the furnace-inside phenomena are, their understanding has advanced, albeit gradually, thanks to the findings of the dismantling investigation, basic laboratory tests, information from various sensors on operating furnaces, and effective use of mathematical models. Of these means, mathematical models for blast furnaces are very

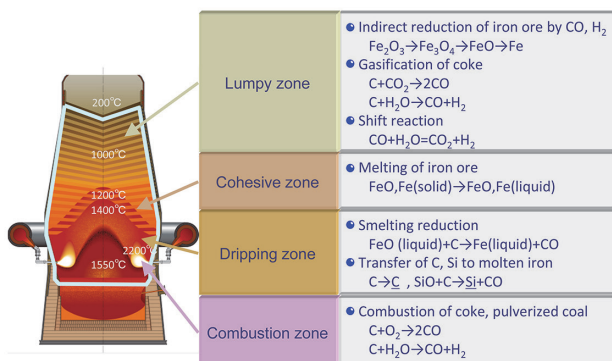


Fig. 1 Transport phenomena in blast furnace

effective at clarifying complicated phenomena taking place inside blast furnaces because by using them it is possible to mathematically express the material movement, heat flow, and the transfer of kinetic momenta, etc., and thus to quantify the material movement inside the furnace.

This present paper outlines the mathematical models for blast furnaces, in the development of which we participated, and presents examples of their applications to the operation of real furnaces.

## 2. Outlines of Mathematical Models for Blast Furnaces and Examples of Calculation Results

### 2.1 Analysis of flow of raw materials, gas and liquid, heat Transfer, and reactions inside blast furnaces<sup>1)</sup>

Various mathematical models have been developed regarding the operation of blast furnaces. At the beginning, they were one-dimensional steady state models, but as the processing speed of computers increased, one-dimensional unsteady state, two-dimensional steady state, and finally three-dimensional unsteady state models were devised. The models presented herein are three-dimensional unsteady state models.

#### 2.1.1 Basic equations

Figure 2 illustrates the configuration of the developed three-dimensional unsteady state model. It deals with the furnace inside space except the hearth, to which hot metal and slag drip down, and comprises the following basic equations on the material balance, the energy balance, and the balance of kinetic momenta of the gas, solid, and liquid phases:

\* Chief Researcher, Dr.Eng., Ironmaking Research Lab., Process Research Laboratories/Mathematical Science & Technology Research Lab., Advanced Technology Research Laboratories  
20-1 Shintomi, Futtsu City, Chiba Pref. 293-8511

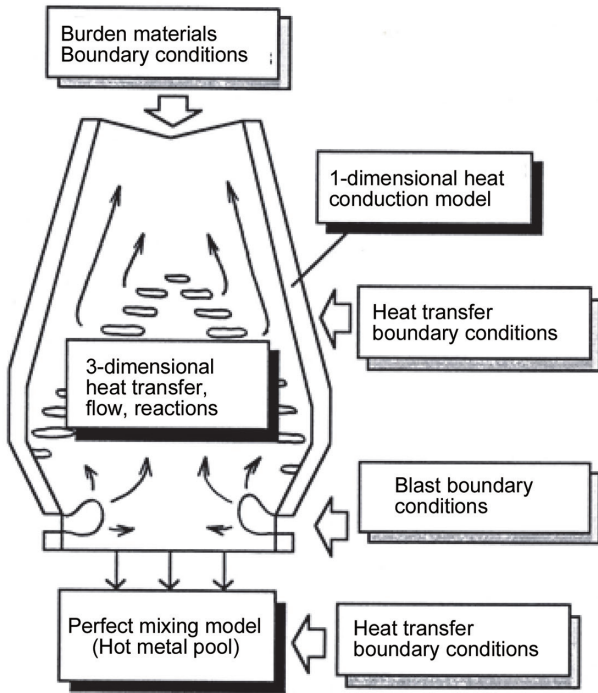


Fig. 2 Schematic diagram of 3-dimensional mathematical model for blast furnace<sup>1)</sup>

$$\frac{\partial(\varepsilon_k \rho_k \omega_{kn})}{\partial t} + \nabla \cdot (\varepsilon_k \rho_k \omega_{kn} \mathbf{u}_k) = \varepsilon_k \nabla \cdot (\rho_k D_k \nabla \omega_{kn}) + RW_{kn}; \quad (1)$$

$$\frac{\partial(\varepsilon_k \rho_k)}{\partial t} + \nabla \cdot (\varepsilon_k \rho_k \mathbf{u}_k) = \sum_n RW_{kn} \quad (2)$$

$$RW_{kn} = M_n \sum_N Rate_N \cdot a_{knN};$$

$$\frac{\partial(\varepsilon_g \rho_g \mathbf{u}_g)}{\partial t} = -\varepsilon_g \nabla P - \varepsilon_g (f_1 + f_2 | \varepsilon_g \rho_g \mathbf{u}_g |) (\varepsilon_g \rho_g \mathbf{u}_g) \quad (3)$$

$$f_1 = 150 \left( \frac{1 - \varepsilon_g}{\varepsilon_g d_p} \right) \frac{\mu_g}{\varepsilon_g \rho_g}, \quad f_2 = 1.75 \left( \frac{1 - \varepsilon_g}{\varepsilon_g d_p} \right) \frac{1}{\varepsilon_g^2 \rho_g};$$

$$u_{xs} = B \frac{\partial u_{ys}}{\partial x}, \quad u_{zs} = B \frac{\partial u_{ys}}{\partial z}; \quad (4)$$

$$u_{yl} = const., \quad u_{xl} = u_{zl} = 0; \quad (5)$$

$$\frac{\partial(\varepsilon_k \rho_k C_p T_n)}{\partial t} + \nabla \cdot (\varepsilon_k \rho_k C_p T_n \mathbf{u}_k) \quad (6)$$

$$= \varepsilon_k \nabla \cdot (k_k \nabla T_k) - \sum_m \{ \alpha_{k-m} U_{k-m} (T_m - T_k) \} + RH$$

$$RH = \sum Rate_N (-\Delta H_N) \eta_{kN}.$$

Here, the symbols are as follows:  $\varepsilon$  is volume fraction;  $\rho$  bulk density;  $\omega$  weight fraction;  $\mathbf{u}$  flow rate;  $D$  diffusion coefficient;  $M$  molecular weight;  $Rate$  reaction rate;  $a$  stoichiometric coefficient;  $P$  pressure;  $d_p$  particle diameter;  $\mu$  viscosity;  $C_p$  specific heat;  $T$  temperature;  $B$  a constant;  $U$  heat transfer coefficient;  $\Delta H$  enthalpy change due to reaction;  $\eta$  heat distribution ratio; and  $\alpha$  effective area of contact. The subscripts are used as follows:  $k$  is replaced by  $g$ ,  $s$ , and  $l$ , where  $g$  indicates gas,  $s$  indicates solid, and  $l$  indicates liquid;  $n$  is replaced by CO, CO<sub>2</sub>, etc. when gas is involved ( $k$  replaced by  $g$ ), by Fe<sub>2</sub>O<sub>3</sub>, Fe<sub>3</sub>O<sub>4</sub>, etc. when solid is involved, and by Fe<sub>2</sub>O<sub>3</sub>, Fe<sub>3</sub>O<sub>4</sub>, etc. when liquid is involved; and  $N$  is replaced by the reaction numbers 1 to 17 in Table 1 (described later).

Table 1 Reactions considered in mathematical blast furnace model

No.	Reactions
1	3Fe <sub>2</sub> O <sub>3</sub> (s) + CO(g) → 2Fe <sub>3</sub> O <sub>4</sub> (s) + CO <sub>2</sub> (g)
2	Fe <sub>3</sub> O <sub>4</sub> (s) + CO(g) → 3FeO(s) + CO <sub>2</sub> (g)
3	FeO(s) + CO(g) → Fe(s) + CO <sub>2</sub> (g)
4	3Fe <sub>2</sub> O <sub>3</sub> (s) + H <sub>2</sub> (g) → 2Fe <sub>3</sub> O <sub>4</sub> (s) + H <sub>2</sub> O(g)
5	Fe <sub>3</sub> O <sub>4</sub> (s) + H <sub>2</sub> (g) → 3FeO(s) + H <sub>2</sub> O(g)
6	FeO(s) + H <sub>2</sub> (g) → Fe(s) + H <sub>2</sub> O(g)
7	C(s) + CO <sub>2</sub> (g) → 2CO(g)
8	C(s) + H <sub>2</sub> O(g) → CO(g) + H <sub>2</sub> (g)
9	FeO(l) + C(s) → Fe(l) + CO(g)
10	C(s) → $\underline{C}$
11	H <sub>2</sub> O(g) + CO(g) = H <sub>2</sub> (g) + CO <sub>2</sub> (g)
12	SiO <sub>2</sub> (l) + C(s) → SiO(g) + CO(g)
13	SiO <sub>2</sub> (s) + C(s) → SiO(g) + CO(g)
14	SiO <sub>2</sub> (s) + 3C(s) → SiC(s) + 2CO(g)
15	SiO(g) + $\underline{C}$ → $\underline{Si}$ + CO(g)
16	Fe(s) → Fe(l)
17	FeO(s) → FeO(l)

### 2.1.2 Handling of phenomena inside blast furnace

The following assumptions were set forth to express the extremely complicated phenomena taking place in a blast furnace.

The components of the gas inside the furnace considered in the model are CO, CO<sub>2</sub>, H<sub>2</sub>, H<sub>2</sub>O, N<sub>2</sub>, etc., those of iron ore and coke are Fe<sub>2</sub>O<sub>3</sub>, Fe<sub>3</sub>O<sub>4</sub>, FeO, Fe, C, SiO<sub>2</sub>, etc., and the reactions listed in Table 1 are included in the model.

Ergun's equation is employed for calculating the pressure drop of the gas inside the furnace. The following assumptions were made for the model: the distribution of the rate of the burden descent (sintered ore, pellets, lump ore, etc.) is obtainable using a kinematic model;<sup>2)</sup> the molten liquid forming in the cohesive zone drips down at a constant speed (because, while the molten liquid of iron and slag form a dispersed phase, the dripping behavior of such a dispersed phase through the coke-packed zones is not clear yet); the coke temperature and the iron ore temperature are the same; and the molten metal temperature and the slag temperature are also the same.

The three-interface unreacted nuclear model<sup>3)</sup> was applied to the reduction reaction of iron ore. As the reaction rate distribution within individual particles has to be considered regarding the gasification of coke, the concept of the Thiele modulus, an effectiveness factor of the catalyst, was adopted, and mass transfer in boundary films was taken into consideration. The combustion in the raceway was not directly dealt with in the model, but the theoretical combustion temperature and the composition and flow rate of the bosh gas were calculated from the composition and temperature of the gas and the pulverized coal blown in through the tuyeres and from the same of the coke coming into the raceway from above.

With respect to the size of the charged materials, the particle size change of iron ore due to reduction degradation and that of coke due to gasification were taken into consideration.

### 2.1.3 Boundary conditions

The chemical compositions of the raw materials charged from the furnace top, their particle size distribution in the radial direction, and the ore/coke distribution in weight were defined as the boundary conditions in the same manner as in real blast furnaces. Other fur-

nance operation conditions such as the volume, temperature, and humidity of the hot blast and the injection amount of pulverized coal were also defined. Setting of these boundary conditions enabled calculation of the distributions inside the furnace of the following: flow rate and concentration of the gas, reduction rate of the ore, coke particle size, etc.

2.1.4 Calculation method

To reflect the shape of a blast furnace, a boundary-fitted grid was used as the computational grid (see Fig. 3). The basic equations were discretized in a staggered grid, and the gas flow was analyzed by the Sola method<sup>4)</sup>. The Point SOR method was used to solve the energy equation and the equations for conservation of mass for gas, solid, and liquid. The fully implicit method was employed for differentiating fluxes and source terms. Figure 4 shows the entire calculation flow.

2.1.5 Comparison of calculation results with observation results

A set of calculation results of the furnace inside condition using the developed model is given in Fig. 5 as examples, and a comparison of the calculated and measured furnace conditions in Fig. 6. It shows that quantitative expression of the complicated phenomena

inside a blast furnace has been made possible by adequate and mathematical expression.

To operate a blast furnace stably, it is essential to clarify the furnace inside condition in unsteady operation. As an example, Fig. 7 compares the calculated and actually recorded blow-in operation conditions of No. 5 BF of Wakayama Works. The calculated values of the composition and temperature of gas at the top, hot metal temperature, and refractory temperature agreed well with the actually measured ones, which verifies the capability of the developed model to predict the furnace behavior in unsteady operation with sufficient accuracy.

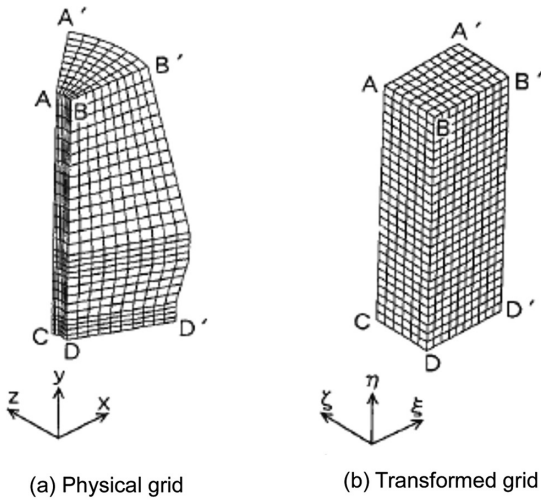


Fig. 3 Grid system<sup>1)</sup>

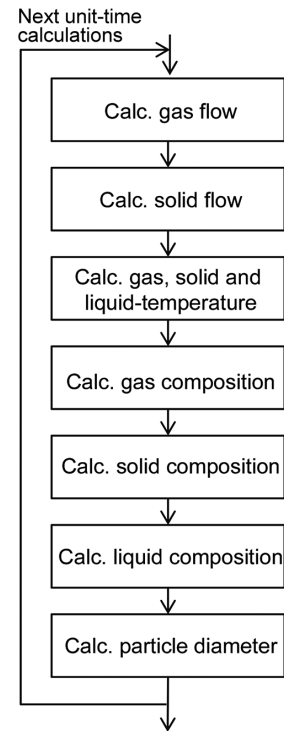


Fig. 4 Solution procedure diagram<sup>1)</sup>

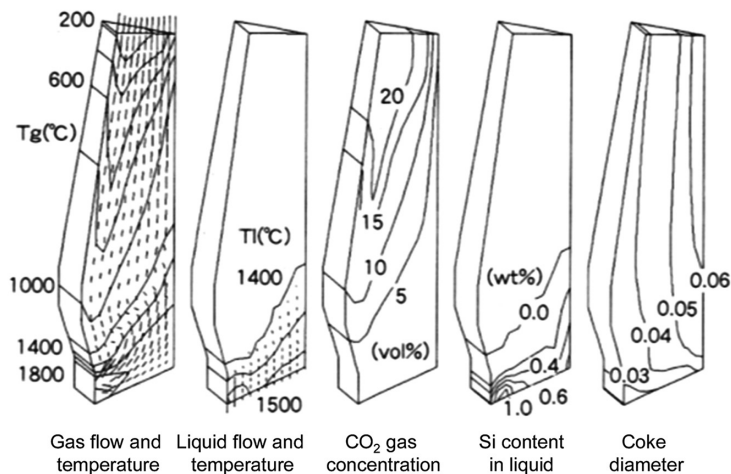


Fig. 5 Computational results of blast furnace by the mathematical model<sup>1)</sup>

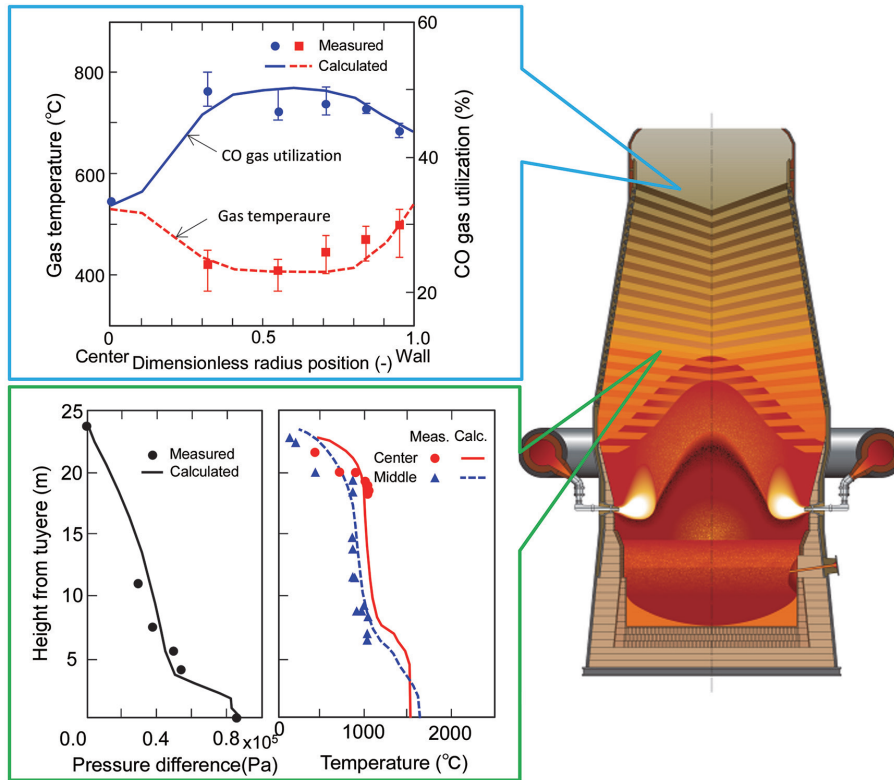


Fig. 6 Comparison of measured and calculated results of Wakayama No. 5 BF (example)<sup>1)</sup>

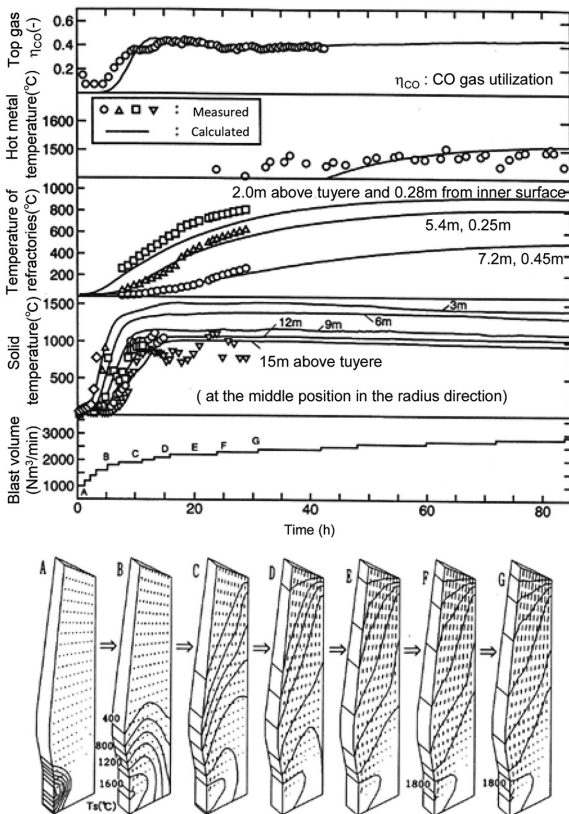


Fig. 7 Calculation results of blow-in operation of Wakayama No. 5 BF<sup>1)</sup>

2.2 Model for reaction analysis in consideration of layered burden structure<sup>5)</sup>

Low coke rate, or low reducing agents' rate operation, has been pursued for purposes such as dealing with the price increase of the raw materials and the change in their supply structure and reduction of CO<sub>2</sub> emission. In low-coke-rate operation, however, the thickness of the coke layers in the furnace decreases, and as a result, pressure drop is feared to increase, but there have only been a small number of theoretical studies on the appropriate thickness of coke layers. To optimally design burden distribution, it is necessary to grasp the stacking condition of the ore layers and coke layers in the furnace. In consideration of this, we developed a calculation model that could express the burden layer structure inside a furnace.

2.2.1 Method for tracing burden layer structure

To express the shape of burden layers in a blast furnace, it is necessary to identify the interfaces between ore layers and coke layers, and trace their descent. Of the various methods for tracing the movement of interfaces, the VOF method<sup>6)</sup> was selected for the model in consideration of the accuracy and computational load. The advection equation of VOF was discretized according to the Crank-Nicolson scheme, and the advection term was discretized using the compressive interface capturing scheme for arbitrary meshes (CIC-SAM)<sup>7)</sup>.

2.2.2 Handling of in-furnace phenomena

The material flow, heat transfer, reactions, etc. inside the furnace were expressed in the developed model basically in the same manner as explained in item 2.1.2 above.

2.2.3 Calculation results

Figure 8 shows a set of calculation results as examples. The images demonstrate that iron ore and coke charged into the furnace from the top in layers descend to the lower part maintaining a struc-

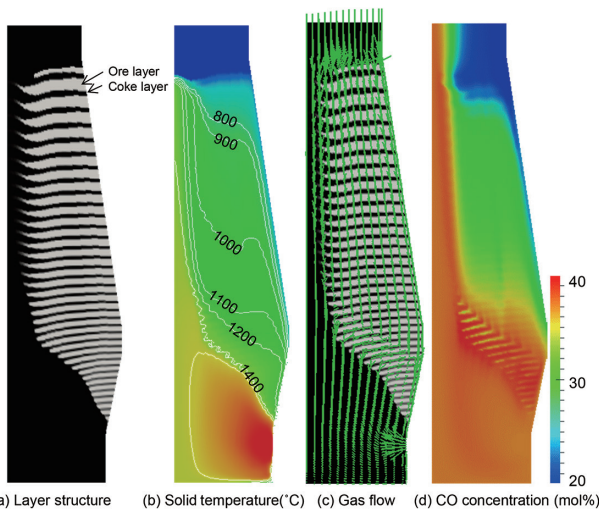


Fig. 8 In-furnace states calculated by mathematical blast furnace model<sup>5)</sup>

ture of distinct layers. The gas is calculated to flow preferentially through coke slits avoiding the cohesive zone of the ore. CO concentration, on the other hand, is estimated to lower in the ore layers owing to the reduction of ore, and increase in the coke layers owing to the gasification of coke. Thus, the model has proved capable of reproducing CO concentration distribution in accordance with the burden layer structure.

### 2.3 Dealing with newly developed raw material<sup>8)</sup>

Aiming at the drastic reduction of the reducing agent rate in hot metal production, various measures have been taken to lower the equilibrium temperature of ore reduction. To accelerate the reactions in blast furnaces and raise the operation efficiency, Nippon Steel & Sumitomo Metal Corporation has endeavored to develop non-fired carbon containing ore agglomerate.<sup>9)</sup> Therefore, the reaction behavior of carbon-containing ore agglomerate in different atmosphere gases was examined and modeled.

#### 2.3.1 Test method

To collect data necessary for modeling the reactions of the ore agglomerate, reaction tests were carried out in atmospheres of different compositions of N<sub>2</sub>, CO, and CO<sub>2</sub>. Specimens of the ore agglomerate were placed in a test vessel, and in the circulating atmosphere of a prescribed composition, heated from room temperature to 1100°C at a rate of 10°C/min, held there for 1 h, and then cooled in an atmosphere of pure nitrogen. During the course of the test, the composition ratios of CO, CO<sub>2</sub>, and N<sub>2</sub> were continuously measured with a mass spectrometer, those of CO and CO<sub>2</sub> with an infrared spectrometer, and the weight change of the ore agglomerate with a strain gauge. The gas flow was also monitored continuously. The rates of reduction and gasification were calculated at different temperatures based on the measured values of the composition and flow rate of the exhaust gas from the vessel.

#### 2.3.2 Reaction model for carbon-containing ore agglomerate

At sectional observation of the specimens, no distinct reaction interfaces were seen in any of those tested in any composition of the N<sub>2</sub>-CO-CO<sub>2</sub> atmosphere. Accordingly, a homogeneous reaction model was adopted as the reaction model for the material. The constants of the reduction rate and the gasification rate at different stages were supposed to exhibit a temperature dependence of the Arrhenius type, and the parameters of the reduction rate and the gasification rate were determined such that the difference between

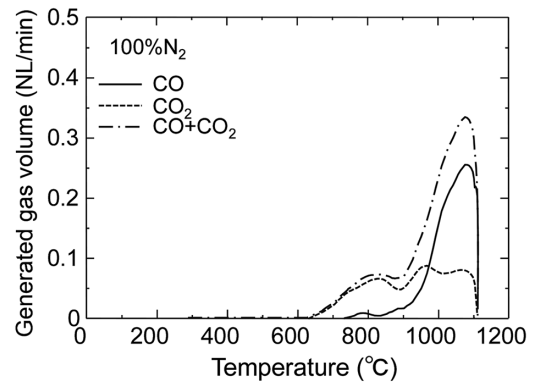


Fig. 9 Gas generation behavior of iron oxide agglomerates<sup>8)</sup>

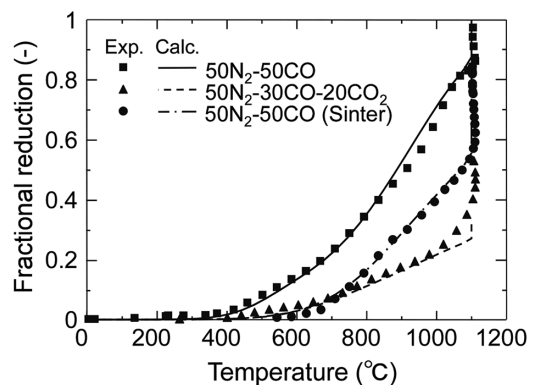


Fig. 10 Comparison of measured and calculated fractional reduction<sup>8)</sup>

the curve obtained through the test and the corresponding curve obtained through calculation was the smallest.

#### 2.3.3 Test result

As an example, Fig. 9 shows the gas generation of the carbon-containing ore agglomerate in a 100%-N<sub>2</sub> atmosphere. It is clear from the graph that the gasification reaction began at a comparatively low temperature of roughly 630°C, and that the gas generated at the beginning of the reaction was composed mostly of CO<sub>2</sub>. Next, Fig. 10 shows the calculated reduction rates and those measured experimentally; they are in good agreement.

The developed model was incorporated in the three-dimensional unsteady state mathematical model for BF operation, and under the condition that the ore agglomerate was used by 50 kg/t-hot metal, the decrease in the consumption of reducing agents was calculated. The estimated decrease in the unit consumption of carbon was 0.36 kg-C/t-hot metal, the same as that obtained through a real test using a real blast furnace of Oita Works<sup>10)</sup>.

### 2.4 Model for predicting refractory erosion at hearth wall and bottom<sup>11)</sup>

#### 2.4.1 Basic equations

This model deals with the refractory and bricks of the coke-packed bed, the coke-free layer, and the hearth bottom in the lower part of the furnace (see Fig. 11). It comprises mass balance equations for solid and liquid, an energy balance equation, and a momentum balance equation as the basic equations:

$$\frac{\partial(\varepsilon\rho)}{\partial t} + \nabla \cdot (\varepsilon\rho\mathbf{u}) = 0; \quad (7)$$

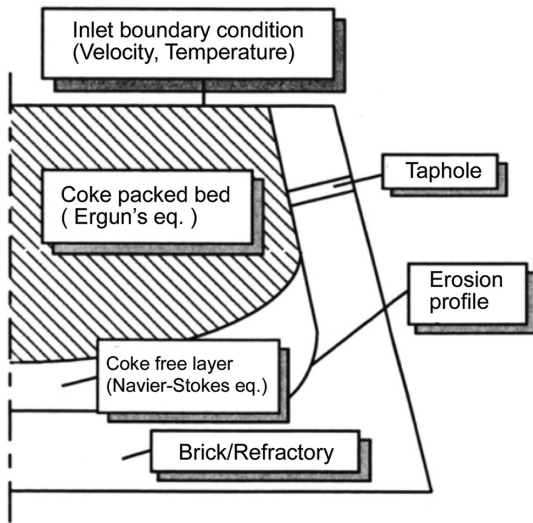


Fig. 11 System of hearth erosion model<sup>11)</sup>

$$\rho \frac{\partial \mathbf{u}}{\partial t} + \rho(\mathbf{u} \cdot \nabla) \mathbf{u} = -\nabla p - \mu \nabla^2 \mathbf{u} + \mathbf{F} = 0; \quad (8)$$

$$\rho \frac{\partial (C_p T)}{\partial t} + \rho(\mathbf{u} \cdot \nabla) C_p T = \nabla(k \nabla T). \quad (9)$$

2.4.2 Boundary conditions

The amount and temperature of the hot metal dripping down into the hot metal pool were defined as the inlet boundary conditions (see Fig. 11), and the upper surface of the bricks was assumed to be heat-insulating. The hot metal flow rate through the tap hole was defined as an outlet boundary condition. An overall heat transfer coefficient was set as the boundary condition at the bottom and outer surfaces of the hearth bricks. Although the space of the coke-packed bed is usually defined based on the result of stress analysis, it is also allowed to define it arbitrarily, which means that it is also possible to examine the effects of the coke-free space in the hearth using the developed model. Refractory fusing temperature was defined, based on the findings of dissection observation of blown-off furnaces, at 1 150°C for carbon bricks and 1 350°C for chamotte bricks.

2.4.3 Calculation method

A boundary-fitted coordinate system was adopted for the model to express the shape of the hearth (see Fig. 12), and a staggered grid was used as the computational grid. The basic equation was discretized on the staggered grid, and the Navier-Stokes equations were solved by the Sola method<sup>4)</sup>. The advective term was discretized using the third-order upwind difference method, and the diffusion term using the second-order central difference method.

The calculation procedures are as follows: first, the distribution of the flow rate of hot metal is obtained by flow analysis; then, the temperature distribution of the entire subject space including hearth bricks is calculated by heat transfer analysis; finally, when the temperature of a brick exceeds a prescribed figure (1 150°C for a carbon brick and 1 350°C for a chamotte brick), the brick in question is considered to have been lost by erosion, and the brick in the corresponding cells is removed, and flow analysis is conducted again assuming that the space is filled with hot metal. The above procedures are repeated until brick erosion does not advance any further. By the above, it is possible to predict the shape of hearth bricks in the state of thermal equilibrium, or their wear condition.

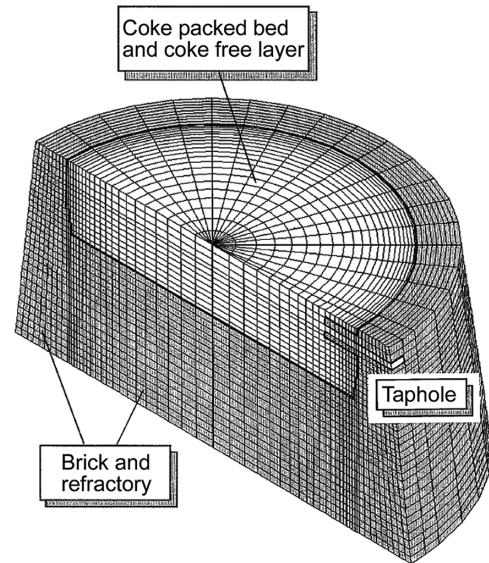


Fig. 12 Boundary fitted coordinate system of computational grid<sup>11)</sup>

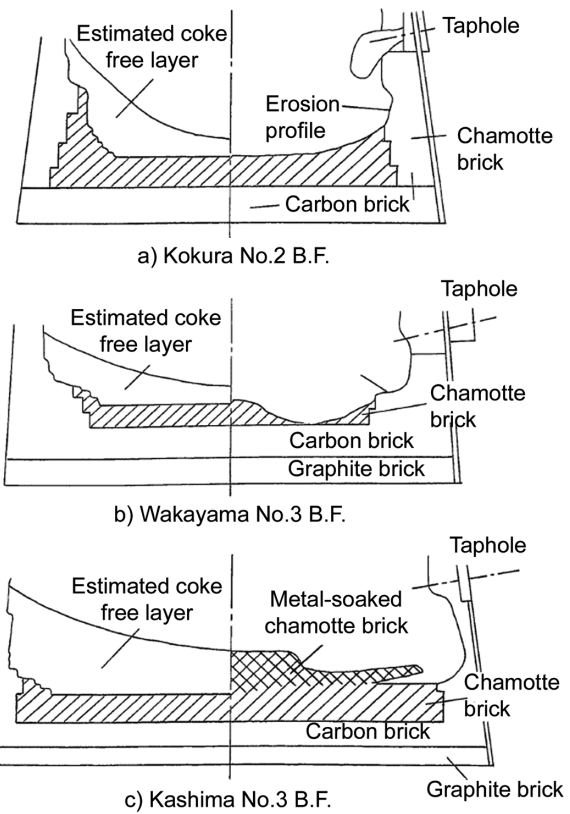


Fig. 13 Comparison of measured and calculated brick erosion profiles of different blast furnaces<sup>11)</sup>

2.4.4 Calculation results

To confirm the prediction accuracy of hearth brick erosion by the developed model, the calculated final hearth brick shape was compared with the sectional measurement result of a real furnace after blow-off; Fig. 13 shows the comparison. By the model calcula-

tion, the hot metal was assumed to be supplied from above the subject space at a constant temperature and at an even flow rate. Here, the shape of the coke-packed bed was defined based on the result of stress analysis. The calculated brick erosion shape agreed well with the measurement at the dissection of the blown-off furnace, which verifies the applicability of the developed model to the prediction of hearth brick erosion in real blast furnaces.

### 3. Conclusion

Mathematical models capable of expressing the phenomena in blast furnaces have been developed: one is a three-dimensional unsteady state model of in-furnace ore reduction reactions and the other is a model for predicting the wear of the hearth wall and bottom bricks. With the developed models it is possible to reproduce or predict various in-furnace phenomena such as the furnace inside condition during steady operation, the change in furnace inside condition

during the unsteady operation after blow-in, and the wear of bricks of the hearth wall and bottom. In appreciation of these advantages, they are being used for the operation analysis of blast furnaces in commercial operation.

### References

- 1) Takatani, K., Inada, T., Ujisawa, Y.: ISIJ Int. 39 (10), 15 (1999)
- 2) Nedderman, R. M., Tuzun, T.: Power Technol. 22, 243 (1979)
- 3) Spitzer, R. H., Manning, F. S., Phillbrook, W. O.: Trans. Metall. Soc. AIME. 236, 1715 (1966)
- 4) Hirt, C. W., Nichols, B. D., Romero, N. C.: Los Alamos. LA-5852, 1975
- 5) Nishioka, K., Ujisawa, Y., Takatani, K.: CAMP-ISIJ. 25, 957 (2012)
- 6) Hirt, C. W., Nichols, B. D.: J. Comp. Phys. 39, 201 (1981)
- 7) Ubbink, O., Issa, R.: J. Comp. Phys. 100, 25 (1992)
- 8) Nishioka, K., Sakai, H., Higuchi, K.: CAMP-ISIJ. 27, 682 (2014)
- 9) Naito, M. et al.: Tetsu-to-Hagané. 87, 357 (2001)
- 10) Yokoyama, H. et al.: ISIJ Int. 52, 2000 (2012)
- 11) Takatani, K., Inada, T., Takata, K.: ISIJ Int. 41 (10), 1139 (2001)



Koki NISHIOKA  
Chief Researcher, Dr.Eng.  
Ironmaking Research Lab., Process Research Laboratories  
Mathematical Science & Technology Research Lab.,  
Advanced Technology Research Laboratories  
20-1 Shintomi, Futtsu City, Chiba Pref. 293-8511



Yutaka UJISAWA  
General Manager, Head of Div., Dr.Env.Eng.  
Experimental Blast Furnace Project Div.  
Process Research Laboratories



Kouji TAKATANI  
Former Advisor, Dr.Eng.  
R & D Laboratories